

Automatic receptor trafficking assay analysis using machine learning

Louis Piloco, Samuel V. Alworth, Hansang Cho, James SJ Lee
SVision LLC, 3633 136th PI SE, Suite 300, Bellevue, WA 98006 USA



Introduction

The spatial temporal dynamics of surface receptors is a common phenotype of interest in neuroscience imaging assays, and is important to inter cellular communication and brain function. The assay result depends on the quantitative characterization of small receptor clusters just a few pixels in diameter in an image. The subcellular phenotype often exhibits weak and unstable signal that is sensitive to noise and variations. This imposes a critical limitation on the image based assay outcomes.

We have previously validated that a subcellular object detection method using confidence maps could enable highly accurate and consistent quantitative analyses of the synaptic vesicle recycling assay. We extended the approach for broad applications by supplementing the validated approach with a learning module. This allows the user to modify and optimize the approach automatically for different applications using a drawing tool on images directly without programming. We previously validated that the learning module could achieve the same high level of accuracy and consistent performance as the validated method using images from a synaptic vesicle recycling assay as well as the standard Transfluor high content screening assay.

We further validate the effectiveness of the learning module using neurotransmitter trafficking image sets provided by our collaborators at the MassGeneral Institute for Neurodegenerative Disease. Our hypothesis is that the learning module will have similar results to that of a commercially available benchmark. We used detection sensitivity, positive predictive value, and segmentation mask accuracy as the performance metrics. In addition, the experimental metrics are reported and compared. We reject the hypothesis with statistical significance. We conclude that the learning module, which can be programmed through drawing, achieves significantly better performance than the commercial benchmark.

Learnable Detection Method

The learnable detection method generates high confidence detection regions by applying structure-guided image processing operations. The structure-guided operations inherently normalize large intensity fluctuations in images to detect small image features, such as common subcellular phenomena. Structure-guided region detection does not introduce phase shift or blurring effect. It is a simple, fast and general method for small object

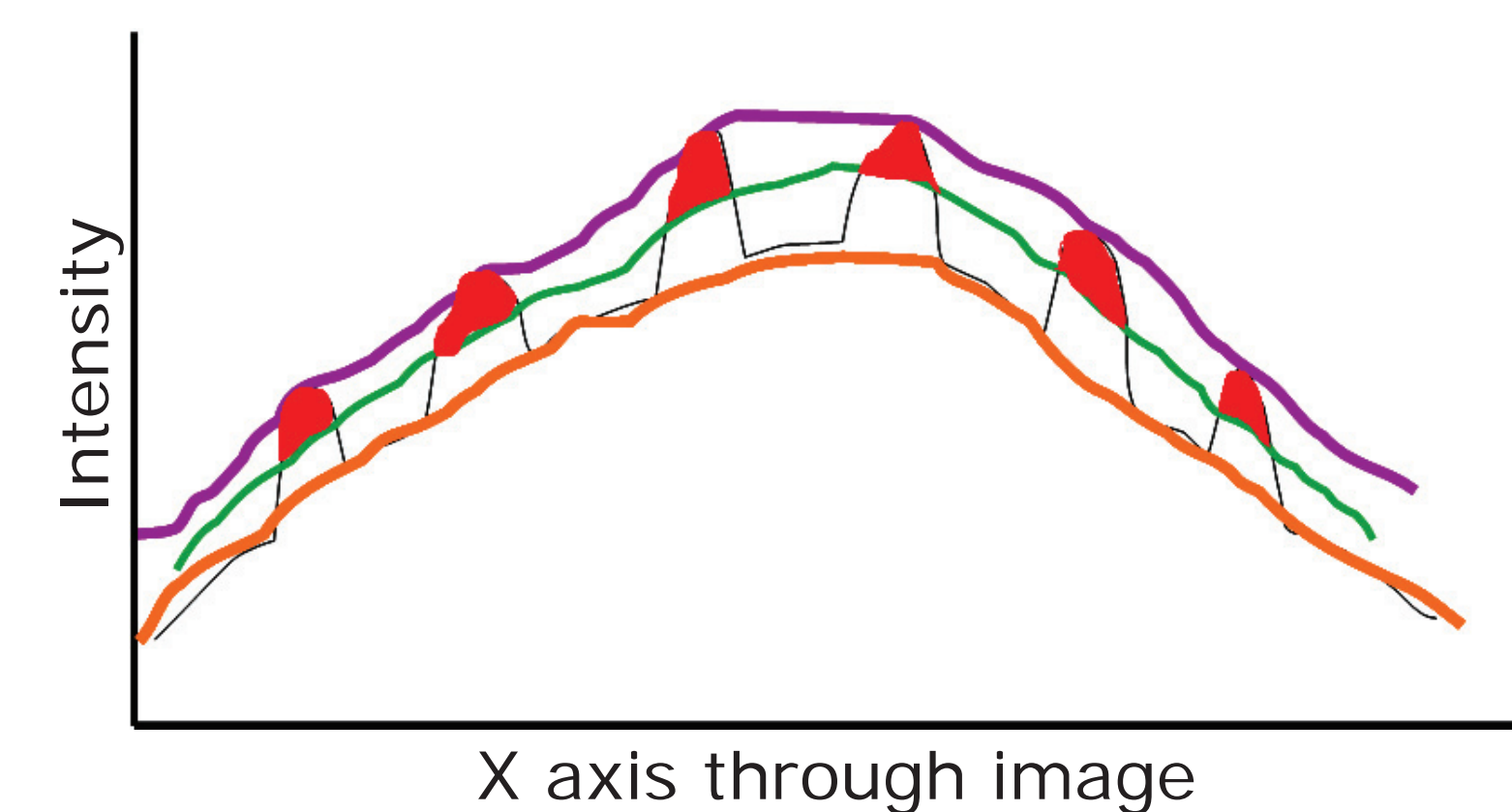
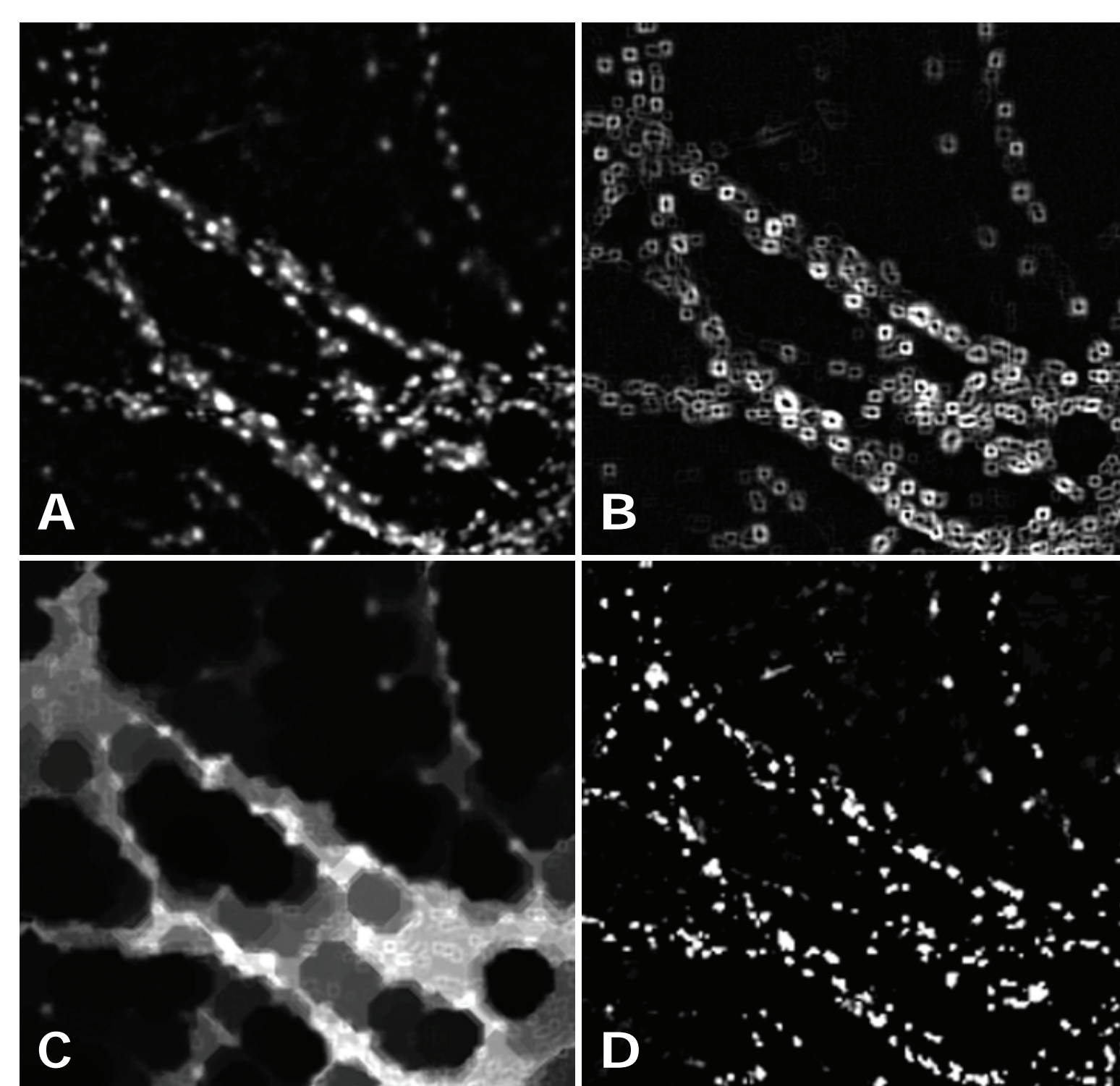


Fig 1. This illustrated example shows how structure-guided processing performs background correction and enhances small features. A) Applying grayscale morphological closing to the input image to generate the closed image (purple), B) Applying grayscale morphological opening to the input image to generate the opened image (orange), C) generating the offset image by averaging the closed image with the opened image and adding an offset (green), and D) subtracting the offset image from the original image (red regions). Figure 2A shows an example enhanced image.

Original grayscale profile	Image profile of average opening & closing plus offset
Image profile after closing operation	Preliminary detection regions
Image profile after opening operation	

Fig 2. The learnable detection method then performs region partition using morphological dilation. The corrected image (A) is dilated to generate expanded regions in x,y that have the same intensity peaks as the corrected image. Subtracting this image from the corrected image generates region boundaries for the peaks in the corrected image (B). A larger dilation parameter will group neighboring peaks together, while a smaller dilation will separate them. To generate the final confidence map (D) a closing operation is performed on the corrected image, and the partition boundaries are added to it (C). Image C is subtracted from the corrected image (A) to produce the confidence map (D). The confidence map can be thresholded to produce the final segmentation mask.



Teaching Interface

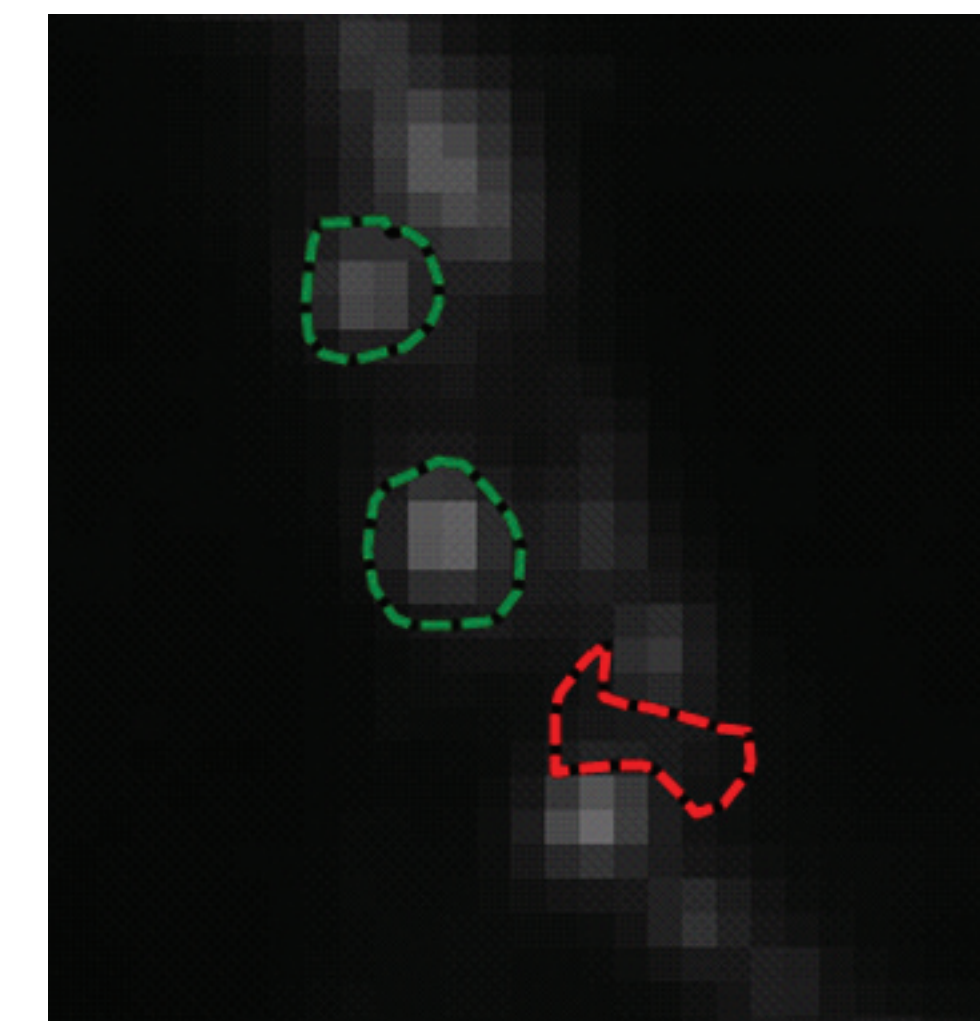
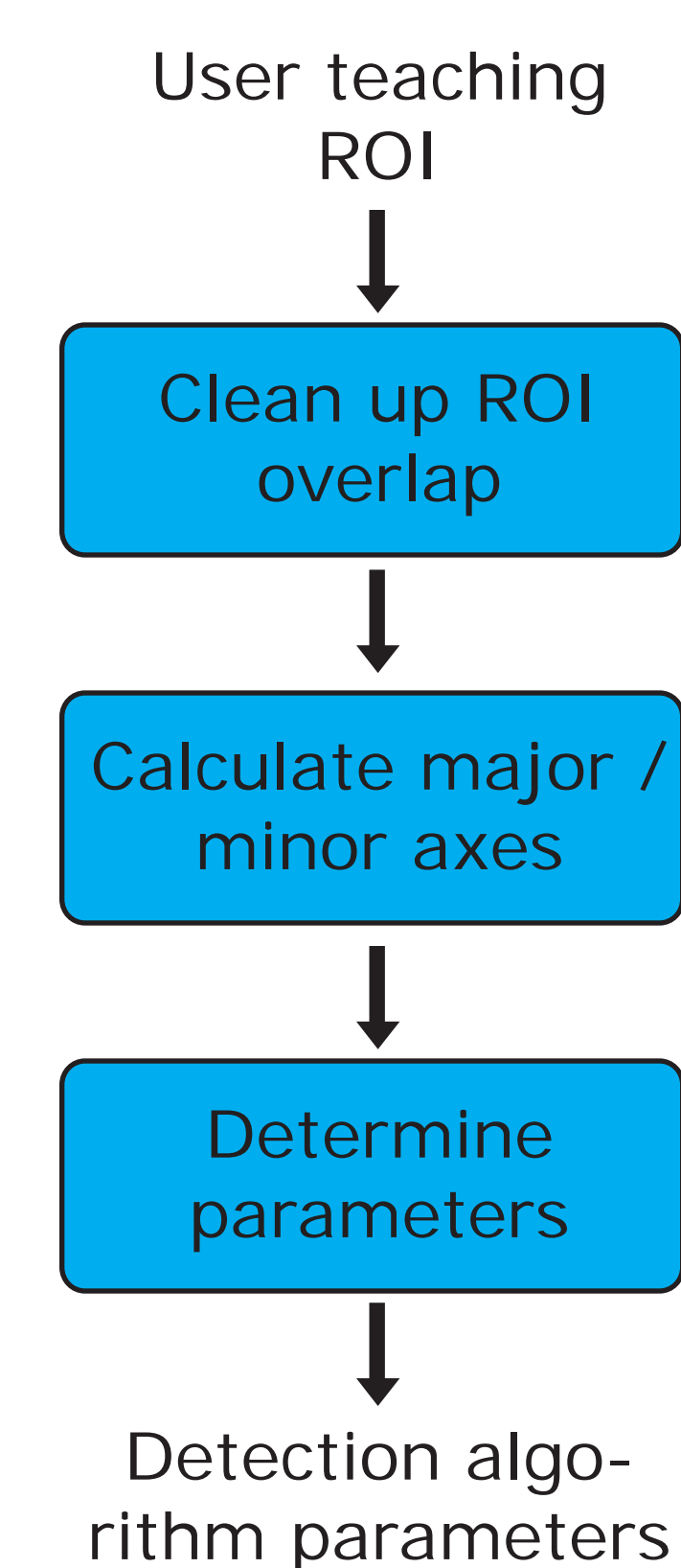


Fig 3. The two parameters required by the learnable detection method can be set by user drawing. Green regions of interest (ROIs) indicate the types of spot patterns desired for enhancement, and red ROIs indicate the patterns for suppression. The learning module maps the size of interest from these ROIs to configure the two detection method parameters.

Fig 4. The method flow chart illustrates the steps in the algorithm parameter determination from user teaching ROI. The first step removes "suppression pattern" ROI regions overlapping with "enhancement pattern" regions. Next the major and minor ROI axes are calculated for both ROI sets. The background correction parameter is the maximum between the minimum minor axis of all suppression ROIs and the maximum major axis of all enhancement ROIs, or the maximum major axis of all enhancement ROIs plus an offset.



Materials and Methods

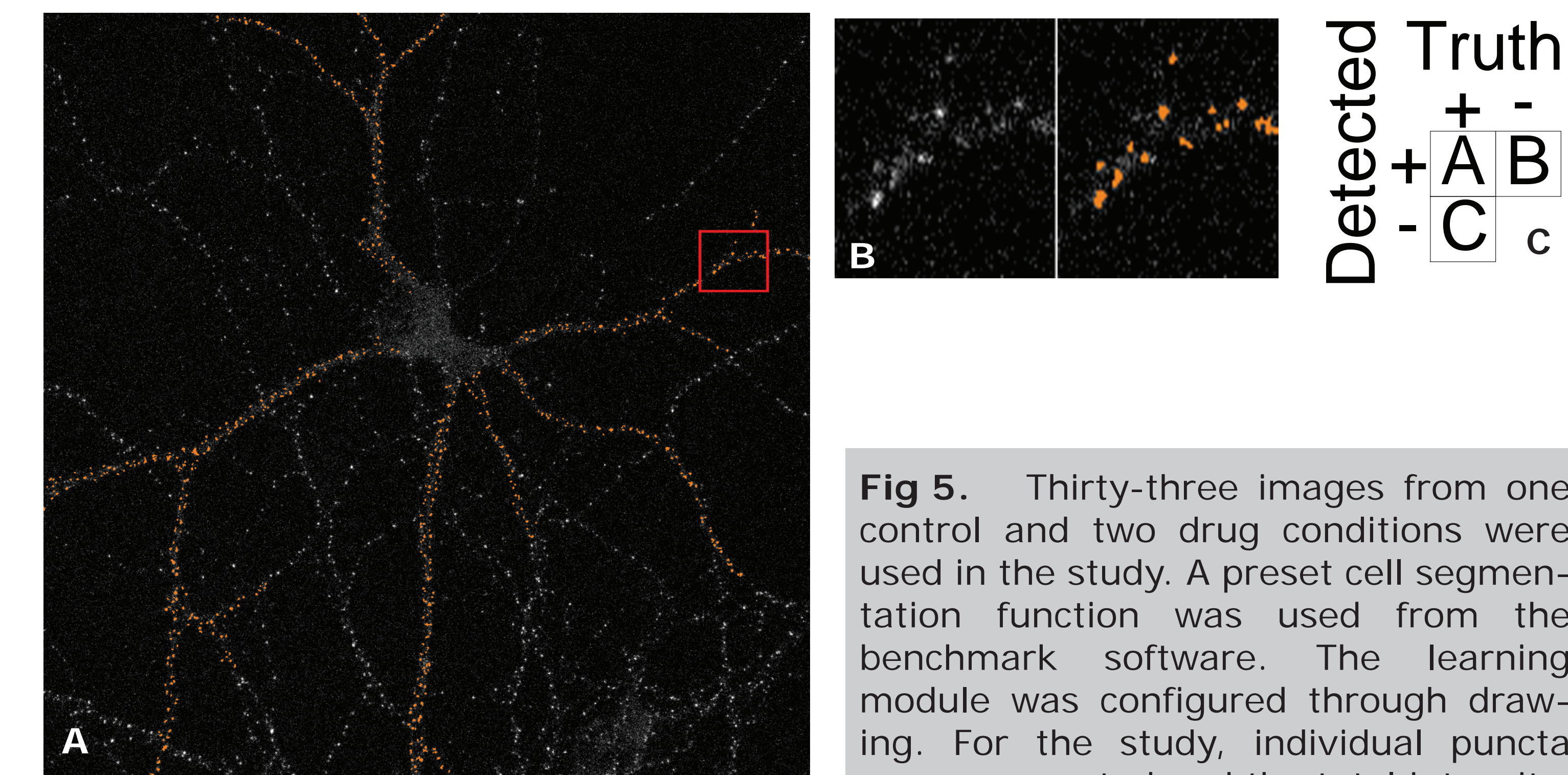


Fig 5. Thirty-three images from one control and two drug conditions were used in the study. A preset cell segmentation function was used from the benchmark software. The learning module was configured through drawing. For the study, individual puncta were segmented and the total intensity

for each puncta was reported. Fig. 5.A shows a representative image with learning module detection mask overlain. Fig. 5.B shows individual puncta appearance with and without the mask overlay. For this study, the two methods are compared in terms of their detection sensitivity, positive predictive value and segmentation accuracy. Dendritic "valid" regions for the comparison were created programmatically using SVCell (SVision LLC). Segmentation accuracy was performed on a stratified sample of the objects (20 per image). "Truth" was independently prepared manually with no knowledge of the learning module algorithm. Fig. 5.C shows the relationship of true and detected objects for the sensitivity and PPV study. The truth is comprised by objects in set A and C. Detected objects by sets A and B. Sensitivity is defined as $A / (A+C)$ and PPV is defined as $A / (A+B)$. The learning module and the benchmark are tested independently. Segmentation error is defined as the pixel count of the exclusive OR of the detected and truth masks, divided by the pixel count of the truth mask (limiting the maximum value to 1).

Results

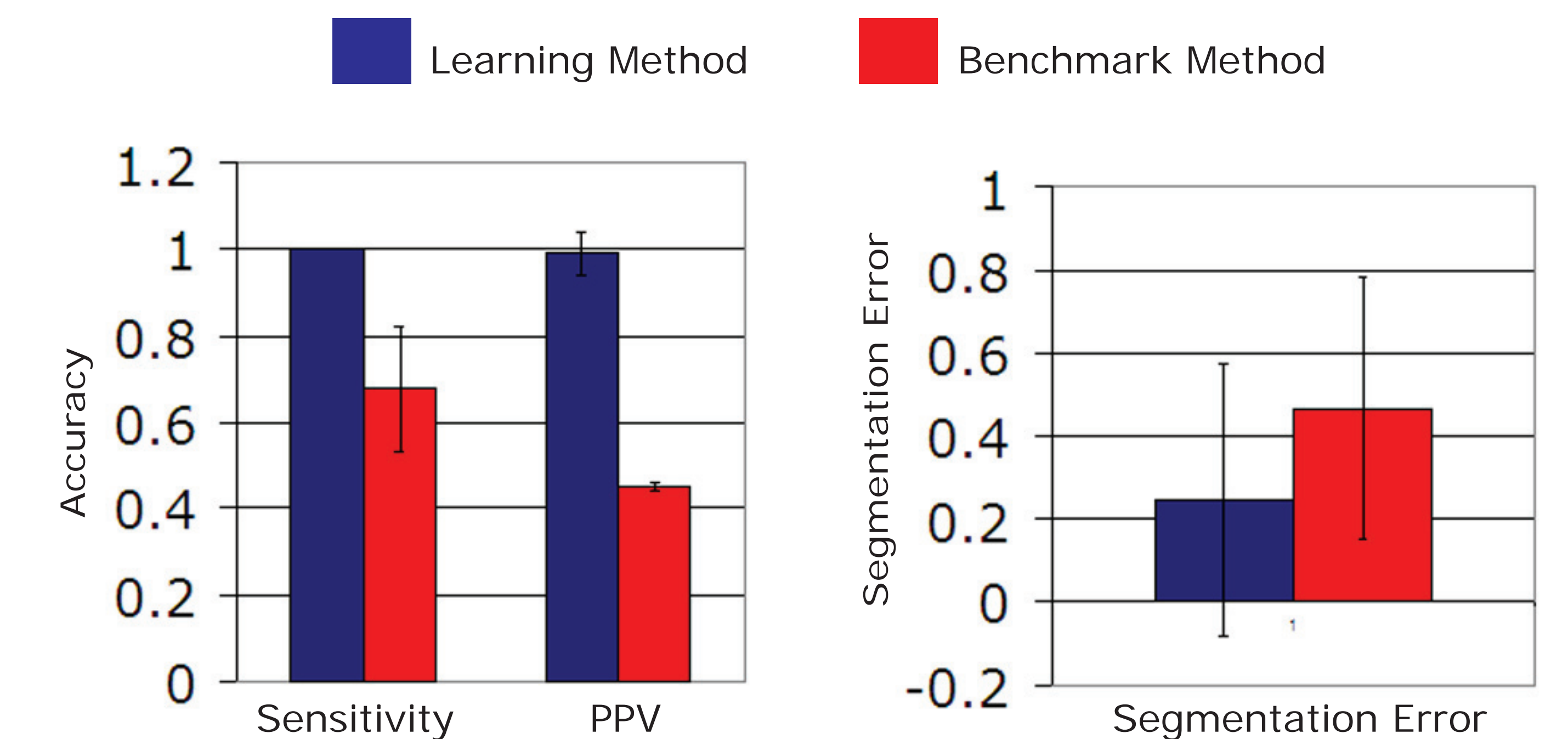


Fig. 6. The learning method has statistically significantly superior analysis performance to the benchmark in terms of sensitivity, positive predictive value and segmentation error. The results are significant using a student's t-test (two sided, unequal variance with one tail) at the $p = 5.44 \times 10^{-15}$, 6.553×10^{-35} , and 5.465×10^{-33} for the sensitivity, positive predictive value and segmentation error studies respectively.

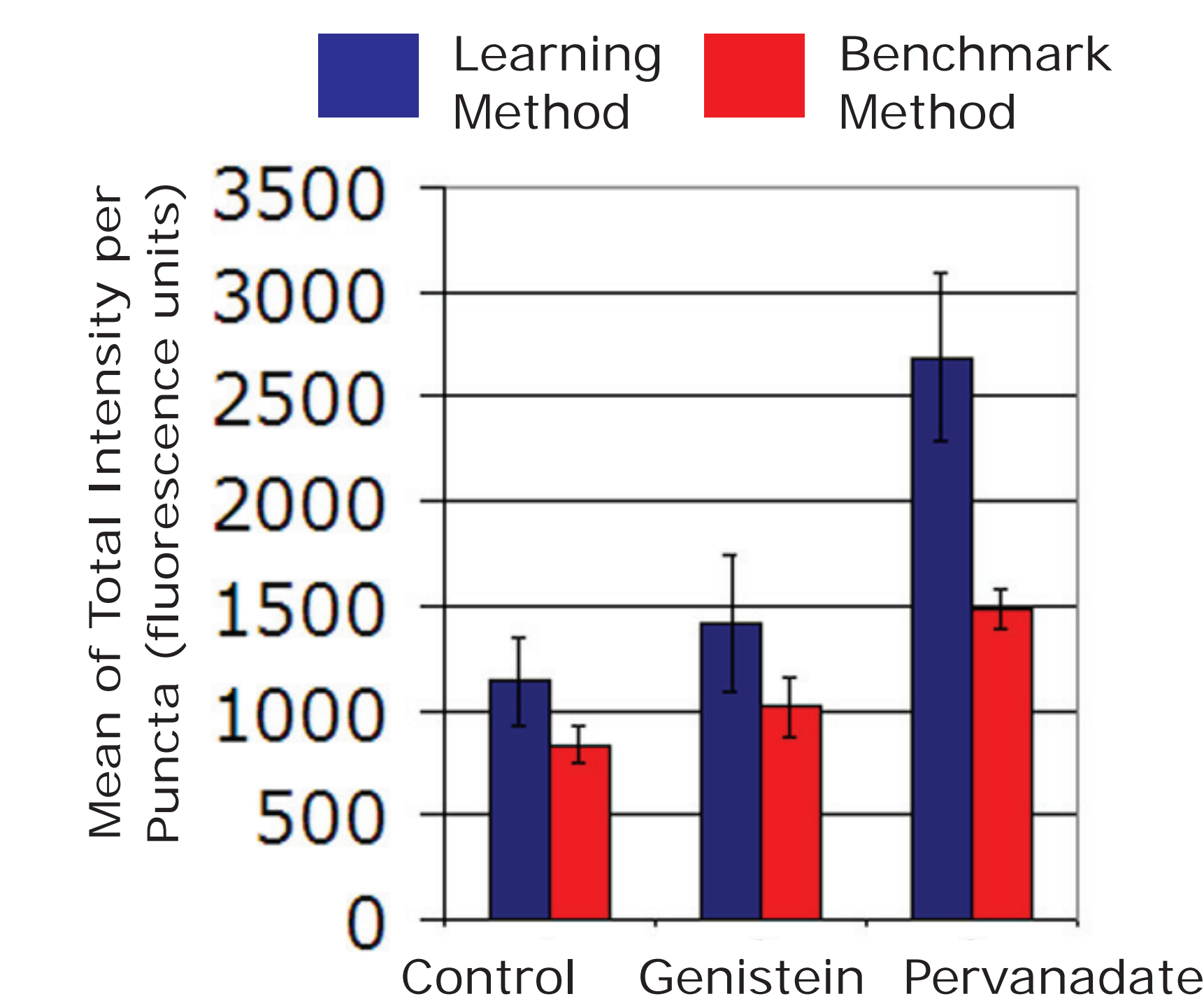


Fig. 7. The learning method has a better outcome in terms of the experimental result. Both methods see the greatest response in the Pervanadate condition, corresponding to the published literature¹. However, the learning method detected response is much stronger. Using Multivariate Analysis of Variance (MANOVA) the learning method detects differences with a p value of 1.248×10^{-10} , while the benchmark method has a p value of only 0.0175.

Conclusion

The validated method was proven to be highly sensitive, specific and consistent on previous, target subcellular assays. However, the validated algorithm, a version of the watershed method, is difficult to make learning enabled and is slow. In a previous study we validated that the new learning method did not have significantly different performance from the validated method for the benchmark assays. In this study we have compared the learning method to "off the shelf" commercially available software with a preset algorithm for puncta detection. The learning method results are significantly and considerably better than the benchmark for this image set. This underscores the benefits of teachable software, where the user can configure the algorithm for their own applications, resulting in better performance.

Literature Cited

Hallet PJ, Spoelgen R, Hyman BT, Standaert DG, Dunah AW.2006. Dopamine D1 Activation Potentiates Striatal NMDA Receptors by Tyrosine Phosphorylation-Dependent Subunit Trafficking. The Journal of Neuroscience, April 26, 2006 • 26(17):4690–4700

Acknowledgements

This research was supported in part by grant no. 2R44MH075498 from the National Institute of Mental Health.